Optimal Power Flow with State Estimation In-the-Loop for Distribution Networks

Yi Guo, *Student Member, IEEE,* Xinyang Zhou, *Member, IEEE,* Changhong Zhao, *Member, IEEE,* Lijun Chen, *Member, IEEE,* and Tyler H. Summers, *Member, IEEE*

***Abstract*—We propose a framework for integrating optimal power flow (OPF) with state estimation (SE) in-the-loop for distribution networks. Our approach combines a primal-dual gradient-based OPF solver with a SE feedback loop based on a limited set of sensors for system monitoring, instead of assuming exact knowledge of all states. The estimation algorithm reduces uncertainty on unmeasured grid states based on a few appropriate online state measurements and noisy "pseudo-measurements". We analyze the convergence of the proposed algorithm and quantify the statistical estimation errors based on a weighted least squares (WLS) estimator. The numerical results on a 4521-node network demonstrate that this approach can scale to extremely large networks and provide robustness to both large pseudo measurement variability and inherent sensor measurement noise.**

***Index Terms*—optimal power flow, state estimation, feedback control, large-scale networks, voltage regulation, distribution networks and power systems.**

I. Introduction

The increasing penetration of distributed energy resources (DERs) has provided more flexibility to better explore the benefits of advanced smart grid technologies in distribution networks. As the heterogeneous control strategies of grid-connected elements dominate distribution networks, many of the customers will become active and motivated end-users to optimize their own power usage via optimal power flow (OPF) methods [1]–[5]. This requires the power system control scheme to have real-time knowledge about the structure and state of the distribution network (e.g., operation states, netload variation, device dynamics, network topology, etc.), and to provide the corresponding real-time responses (e.g., optimal control inputs. set-points of DERs, etc.) for safe and efficient operation. However, the current distribution network control paradigm cannot satisfy the above requirement due to an under-developed information feedback mechanism, and high expense of real-time system states measurement. Future distribution systems will require more sophisticated and tightly integrated control, optimization, and estimation methods for these issues.

Most OPF methods for distribution networks in the literature assume complete availability of network states to implement various optimal control strategies [6]–[17]. However, in practice network states must be estimated with a monitoring system from noisy measurements, which itself is a challenging problem due to the increasingly complex, extremely large-scale, and nonlinear time-varying nature of emerging networks. To solve these issues, the recently proposed OPF frameworks [18]–[21] leverage measurement feedback-based online optimization method to loop the physical measurement information back to OPF controllers, which adapt the OPF decisions to real-time data to mitigate the effects of inherent disturbances and modelling errors. It is unrealistic to have real-time physical measurements of system states at every corner of distribution networks due to heavy communication burdens, end-user privacy concerns, and high costs.

In this paper, we propose a more general framework than the existing OPF approaches, which tightly integrates state estimation (SE) techniques [22]–[26] into online OPF control algorithms for distribution networks. This OPF with SE in-the-loop framework allows us to utilize a limited set of sensor measurements together with a power system state estimator instead of exact knowledge of network states. The power system state estimator, which may include data from the Supervisory Control and Data Acquisition (SCADA) system, phasor measurement units (PMUs), topology processor and pseudo measurements[1], provides the best available information about network states [22], [23], [25], [27]–[29] and in-turn enables implementation and enhances the performance of OPF controllers. Our approach allows OPF decisions to adapt in real-time time-varying stochastic DERs and loads, and compensates for disturbances and modelling errors, since SE results utilize measurement data from the actual nonlinear system dynamics.

A preliminary version of this work appeared in [30], and here we significantly expand the work in several directions. The main contributions are as follows:

This material is based on work supported by funding from US Department of Energy Office of Energy Efficiency and Renewable Energy Solar Energy Technologies Office under contract No. DE-EE-0007998 and the National Science Foundation under grant CMMI-1728605. *(Corresponding author: Xinyang Zhou).*

Y. Guo and T.H. Summers are with the Department of Mechanical Engineering, The University of Texas at Dallas, Richardson, TX 75080, USA, email: {yi.guo2, tyler.summers}@utdallas.edu.

X. Zhou is with Department of Power System Engineering, National Renewable Energy Laboratory, Golden, CO 80401, USA, email: xinyang.zhou@nrel.gov.

C. Zhao is with Department of Information Engineering, the Chinese University of Hong Kong, HKSAR, China, email: chzhao@ie.cuhk.edu.hk.

L. Chen is with College of Engineering and Applied Science, The University of Colorado, Boulder, CO 80309, USA, email: lijun.chen@colorado.edu.

[1]Due to the lack of real time measurement and stochasticity nature of power netloads in distribution system state estimation, the nodal power injections are measured by their nominal load-pattern (i.e., the real value plus zero-mean random deviations), so-called pseudo-measurement, whose information is derived from the past records of load behaviors [26].

1) We formulate a general convex OPF problem subject to power flow equations and network-wise coupling constraints. To integrate OPF with SE in-the-loop, we propose a primal-dual gradient-based OPF algorithm with state estimation feedback. Instead of requiring full knowledge of all system states, the controller utilizes at every gradient step real-time monitoring information from state estimation results to inform control decisions. Whereas OPF and SE problems for distribution networks have been widely studied individually, none of the existing literature explores the connection and bridge the gap between them. Here we are closing the loop between OPF and state estimation in large-scale distribution networks, which guarantees full availability of state estimates [16], [31]. This allows us to react to real-time information of system states with limited number of deployed sensors. In principle, the framework allows a variety of state estimation methodologies and control strategies in distribution networks. Here, we illustrate the approach through a voltage regulation problem with voltage magnitude estimation in-the-loop.
2) We leverage linear approximations of the AC power flow equations, to facilitate scalable and computationally efficient OPF problems for SE feedback integration [18]–[20]. The voltage profile estimation uses a weighted least squares (WLS) estimator. Convergence of the proposed gradient-based algorithm with state estimation feedback is analytically established. Additionally, we quantify the statistical estimation errors of the WLS estimator. This provides a measure of quality of the SE feedback associated with a particular allocation of sensors across the network.
3) The effectiveness, scalability, flexibility and robustness of the proposed algorithm are demonstrated on a 4521-node multi-phase unbalanced distribution network with 1043 (aggregated) netloads. With only 3.6% voltage measurement deployment, the integrated OPF controller with SE feedback effectively regulates network voltage. The distributed algorithm in [32] using linearized distribution flow (LinDistFlow) enables scaling to extremely large networks. The numerical results also indicate that the proposed OPF controller with SE feedback has excellent performance and robustness to the inherent measurement noise and estimation errors.

II. Optimal Power Flow with State Estimation In-the-Loop

In this section, we propose an OPF solver with state estimation feedback. We first pose a general problem to highlight the overall approach, and in subsequent sections we detail the model, objectives, constraints and state estimator for a certain control and monitoring purpose.

Consider the OPF problem for distribution networks

$$\min_{\mathbf{p},\mathbf{q}} \quad \sum_{i\in\mathcal{N}} C_i(p_i,q_i) + C_0(\mathbf{p},\mathbf{q}), \tag{1a}$$

$$\text{s.t.} \quad \mathbf{g}(\mathbf{r}(\mathbf{p},\mathbf{q})) \le 0, \tag{1b}$$

$$(p_i,q_i) \in \mathcal{Z}_i, \forall i \in \mathcal{N}, \tag{1c}$$

where $C_0(\mathbf{p},\mathbf{q})$ is a cost function capturing system objectives (e.g., cost of deviation of total power injections into the substation from nominal values), the local objective function $C_i(p_i,q_i)$ captures the generation costs, ramping costs, active power losses, renewable curtailment penalty, auxiliary service expenses and reactive compensation (comprising a weighted sum thereof) at node $i \in \mathcal{N}$. We then define a state vector $\mathbf{r}(\mathbf{p},\mathbf{q}) \in \mathbf{R}^M$ denoting (combined) electrical quantities of interests (e.g., voltage magnitude, current injections, power injection at the substation, etc.), which depends on nodal power injections $\mathbf{p} := [p_1,\dots,p_N]^\intercal$ and $\mathbf{q} := [q_1,\dots,q_N]^\intercal$ through AC power flow equations[2]. The constraint function $g : \mathbf{R}^M \to \mathbf{R}^{N_g}$ models network constraints, including voltage magnitude, voltage angle, current injection and line flows. The nodal power injections are constrained to convex and compact feasible sets $\mathcal{Z}_i$.

Problem (1) is typically solved assuming that all system states are available. However, in practice, there is generally a lack of reliable measurement devices and communication infrastructure in distribution networks, rendering these conventional OPF approaches impractical. Therefore, the main challenges for solving (1) in practice involve how to best integrate *estimates* of current system states $\mathbf{r}$ and understanding tradeoffs between SE performance and sensor deployment quality and OPF controller performance. We will tackle these by integrating a state estimation feedback loop with a limited number of sensor measurements. This allows the OPF controller to respond to real-time information and update control decisions despite "blind spots" in the grid. The overall approach is illustrated in Fig. 1.

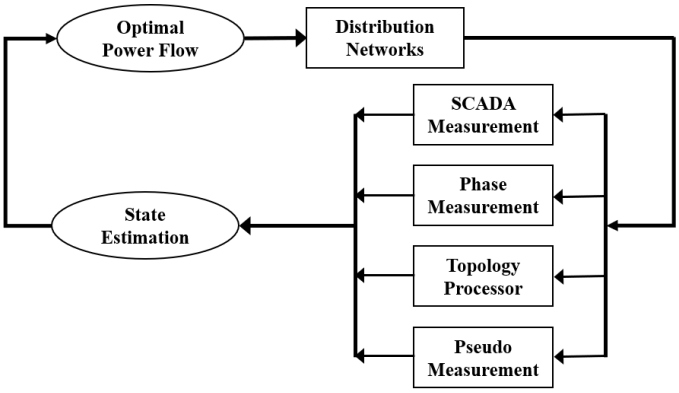

Fig. 1. The concept of solving optimal power flow with state estimation in-the-loop.

In our general framework, the SE techniques may determine the system states using any or all of SCADA measurements, phasor measurement units (PMUs) measurements, pseudo-measurements and topology information to reduce estimation uncertainty. How to fuse different sources of information into OPF formulations remains largely an open question under

[2]The AC power flow relations may represent either full nonlinear power flow, SOCP relaxations, SDP relaxations, or various linearization. The general approach of OPF with SE in-the-loop can be adapted to various (approximate) power flow mappings. In the rest of this paper, we use a linearized power flow model to illustrate the effectiveness of the proposed framework.

exploration. We aim to indicate that there are many possibilities and research direction to potentially improve control and optimization in distribution networks through tight integration with SE. The increasing penetration of renewable energy resources and distributed generators enable the distribution networks with smart features, such as demand response and distributed automation. This allows the networks turn to a more active and complex system with fast dynamics. An efficient, real-time monitoring of distribution networks should be looped into OPF controllers. In the rest of this paper, we take the voltage regulation problem with voltage estimation as an illustrative example, which is based on a few PMU voltage measurements and netload pseudo measurements.

III. Gradient-Based OPF Solver with State Estimation Feedback

A. System Modelling

Consider a distribution network denoted by a directed and connected graph $\mathcal{G}(\mathcal{N}_0, \mathcal{E})$, where $\mathcal{N}_0 := \mathcal{N} \cup \{0\}$ is a set of all "buses" or "nodes" with substation node 0 and $\mathcal{N} := \{1, \ldots, N\}$, and $\mathcal{E} \subset \mathcal{N} \times \mathcal{N}$ is a set of "links" or "lines" for all $(i, j) \in \mathcal{E}$. Let $V_i := |V_i|e^{j\angle V_i} \in \mathbf{C}$ and $I_i := |I_i|e^{j\angle I_i} \in \mathbf{C}$ denote the phasor for the line-to-ground voltage and the current injection at node $i \in \mathcal{N}$. The absolute values $|V_i|$ and $|I_i|$ denote the signal root-mean-square values and $\angle V_i$ and $\angle I_i$ corresponding to the phase angles with respect to the global reference. We collect these variables into complex vectors $\mathbf{v} := [V_1, V_2, \ldots, V_N]^\intercal \in \mathbf{C}^N$ and $\mathbf{i} := [I_1, I_2, \ldots, I_N]^\intercal \in \mathbf{C}^N$. We denote the complex admittance of line $(i, j) \in \mathcal{E}$ by $y_{ij} \in \mathbf{C}$. The admittance matrix $\mathbf{Y} \in \mathbf{C}^{N\times N}$ is given by

$$Y_{ij} = \begin{cases} \sum_{l\sim i} y_{il} + y_{ii} & \text{if } i = j \\ -y_{ij} & (i, j) \in \mathcal{E} \\ 0 & (i, j) \notin \mathcal{E} \end{cases}, \tag{2}$$

where $l \sim i$ indicates connection between node l and node i, and y_{ii} is the self admittance of node i to the ground.

Node 0 is modelled as a slack bus. The other nodes are modelled as PQ buses for which the injected complex power is specified. The admittance matrix can be partitioned as

$$\begin{bmatrix} I_0 \\ \mathbf{i} \end{bmatrix} = \begin{bmatrix} y_{00} & \bar{y}^\intercal \\ \bar{y} & \mathbf{Y} \end{bmatrix} \begin{bmatrix} V_0 \\ \mathbf{v} \end{bmatrix}.$$

The net complex power injection then reads:

$$\mathbf{s} = \text{diag}(\mathbf{v})\Big(\mathbf{Y}^*(\mathbf{v})^* + \bar{y}^*(V_0)^*\Big), \tag{3}$$

where superscript $(\cdot)^*$ indicates the element-wise conjugate of complex vector $\mathbf{v}$.

To facilitate computational efficiency using convex optimization, here we leverage a linearization of (3) as follows:

$$\mathbf{r} = \mathbf{A}\mathbf{p} + \mathbf{B}\mathbf{q} + \mathbf{r}_0,$$

where the parameters $\mathbf{A}$, $\mathbf{B}$ and $\mathbf{r}_0$ can be attained from various linearization methods, e.g., [33]–[36]. Recall that $\mathbf{r} \in \mathbf{R}^M$ represents certain electrical quantities of interests (e.g., voltage magnitude, current injections, power injection at the substation, etc.).

B. OPF Formulation and Primal-Dual Gradient Algorithm

In this section, we introduce a general OPF problem and the pertinent gradient algorithm with idealized measurement feedback[3] from nonlinear power flow to reduce modelling errors. The feasible operating regions $\mathcal{Z}_i$ depend on the terminal properties of various dispatchable devices, e.g., inverter-based distributed generators, energy storage systems or small-scale diesel generators. We make the following assumptions.

Assumption 1. *The feasible regions $\mathcal{Z}_i$ for power nodal injections are restricted to box constraints.*

Assumption 2 (Slater's condition)**.** *There exists a strictly feasible point within the operation region $(\mathbf{p}, \mathbf{q}) \in \mathcal{Z}$, where $\mathcal{Z} := \mathcal{Z}_1 \times \ldots \times \mathcal{Z}_N$, so that*

$$\mathbf{g}(\mathbf{r}(\mathbf{p}, \mathbf{q})) < 0.$$

Assumption 3. *A set of local objective functions $C_i(p_i, q_i), \forall i \in \mathcal{N}$ are continuous differentiable and strongly convex as functions of (p_i, q_i), and their first order derivative are bounded within their operation regions indicated as $(p_i, q_i) \in \mathcal{Z}_i, \forall i \in \mathcal{N}$; The system-wise objective function $C_0(\mathbf{p}, \mathbf{q})$ is continuously differentiable and convex with its first-order derivative bounded. Furthermore, the constraint function g is continuously differentiable and convex with bounded derivatives on its domain.*

The regularized Lagrangian $\mathcal{L}$ for (1) is

$$\mathcal{L} = \sum_{i\in\mathcal{N}} C_i(p_i, q_i) + C_0(\mathbf{p}, \mathbf{q}) + \boldsymbol{\mu}^\intercal \mathbf{g}(\mathbf{r}(\mathbf{p}, \mathbf{q})) - \frac{\eta}{2}\|\boldsymbol{\mu}\|_2^2 \tag{4}$$

where $\boldsymbol{\mu}$ is the dual variable vector associated with the general inequality constraints and we keep the feasible regions $\boldsymbol{\mu} \geq 0$ and $(\mathbf{p}, \mathbf{q}) \in \mathcal{Z}$ implicit. To facilitate proof of convergence, the Lagrangian (4) includes a Tikhonov regularization term $-\frac{\eta}{2}\|\boldsymbol{\mu}\|_2^2$ with a prescribed small parameter η that introduces bounded discrepancy [37]. Then to solve (1) we come to the saddle-point problem

$$\max_{\boldsymbol{\mu}\in\mathbf{R}_+} \min_{(\mathbf{p},\mathbf{q})\in\mathcal{Z}} \mathcal{L}(\mathbf{p}, \mathbf{q}, \boldsymbol{\mu}), \tag{5}$$

which leads to an iterative primal-dual gradient algorithm to reach the unique saddle-point of (5)

$$\mathbf{r}^k = \mathbf{A}\mathbf{p}^k + \mathbf{B}\mathbf{q}^k + \mathbf{r}_0, \tag{6a}$$
$$\mathbf{p}^{k+1} = \left[\mathbf{p}^k - \epsilon\nabla_{\mathbf{p}}\mathcal{L}|_{\mathbf{p}^k,\mathbf{q}^k,\boldsymbol{\mu}^k}\right]_{\mathcal{Z}}, \tag{6b}$$
$$\mathbf{q}^{k+1} = \left[\mathbf{q}^k - \epsilon\nabla_{\mathbf{q}}\mathcal{L}|_{\mathbf{p}^k,\mathbf{q}^k,\boldsymbol{\mu}^k}\right]_{\mathcal{Z}}, \tag{6c}$$
$$\boldsymbol{\mu}^{k+1} = \left[\boldsymbol{\mu}^k + \epsilon\nabla_{\boldsymbol{\mu}}\mathcal{L}|_{\mathbf{r}^k,\boldsymbol{\mu}^k}\right]_{\mathbf{R}_+}, \tag{6d}$$

where $\epsilon \in \mathbf{R}_{++}$ is a constant stepsize to be determined, and the operators $[\cdot]_{\mathcal{Z}}$ and $[\cdot]_{\mathbf{R}_+}$ project onto the feasible set $\mathcal{Z} := \times_{i\in\mathcal{N}}\mathcal{Z}_i$ and nonnegative orthant, respectively. The updates (6) are represented compactly by the mapping

$$\Phi : \{\mathbf{p}^k, \mathbf{q}^k, \boldsymbol{\mu}^k\} \mapsto \begin{bmatrix} \epsilon\nabla_{\mathbf{p}}\mathcal{L}|_{\mathbf{p}^k,\mathbf{q}^k,\boldsymbol{\mu}^k} \\ \epsilon\nabla_{\mathbf{q}}\mathcal{L}|_{\mathbf{p}^k,\mathbf{q}^k,\boldsymbol{\mu}^k} \\ -\epsilon\nabla_{\boldsymbol{\mu}}\mathcal{L}|_{\mathbf{r}^k,\boldsymbol{\mu}^k} \end{bmatrix},$$

[3]The "idealized" refers to the full measurement of vector $\mathbf{r}$ without noise.

so that (6) can be written as

$$\mathbf{x}^{k+1} = \left[\mathbf{x}^k - \epsilon\Phi(\mathbf{x}^k)\right]_{\mathbf{R}_+\times\mathcal{Z}}, \tag{7}$$

where $\mathbf{x}^k := [(\mathbf{p}^k)^\intercal, (\mathbf{q}^k)^\intercal, (\boldsymbol{\mu}^k)^\intercal]^\intercal$. Under Assumption 3, it can be shown [32] that Φ is strongly monotone and Lipschitz continuous, i.e., it satisfies for all feasible points $\mathbf{x}_1$ and $\mathbf{x}_2$ and for some constants $M > 0$ and $L > 0$

$$(\Phi(\mathbf{x}_1) - \Phi(\mathbf{x}_2))^\intercal (\mathbf{x}_1 - \mathbf{x}_2) \geq M\|\mathbf{x}_1 - \mathbf{x}_2\|_2^2, \tag{8}$$

$$\|\Phi(\mathbf{x}_1) - \Phi(\mathbf{x}_2)\|_2^2 \leq L^2\|\mathbf{x}_1 - \mathbf{x}_2\|_2^2. \tag{9}$$

We now have the following result from [30].

Theorem 1. *Consider the primal-dual gradient algorithm* (6) *for the optimization problem* (1) *based on the regularized Lagrangian* (4)*. If the step size* ϵ *satisfies*

$$0 < \epsilon < 2M/L^2, \tag{10}$$

algorithm (6) *converges to the unique saddle point of* (4)*.*

The optimization problem (1) and gradient algorithm (6) are based on a linearized power flow to guarantee its convexity and prove convergence to the saddle point. However, linearization errors cause the solution of (6) to be suboptimal or even infeasible for the system with nonlinear power flow. To address this issue, feedback-based online optimization methods [18], [19], [38] have been leveraged to reduce the effects of modelling error. In particular, by replacing (6a) with following nonlinear power flow

$$\mathbf{r}^k \quad = \quad f(\mathbf{p}^k, \mathbf{q}^k), \tag{11}$$

that obtained from the physical system, these measured values $\mathbf{r}^k$ can be used, instead of an approximate model, to update dual variables in (6d). Convergence to a bounded range of the optimum can be analytically shown for such implementations, and this also facilitates a real-time implementation that can track the time-varying grid conditions [19], [20].

However, one crucial issue of such feedback-based algorithm has been largely overlooked: in practice, there are too few monitoring devices in distribution systems to measure all components of $\mathbf{r}$, and therefore it is not possible to directly implement feedback-based algorithms to solve the problem (1). Our preliminary results [30] demonstrated that limited knowledge of system states can lead the OPF controller to cause constraint violations.

To enable an implementation of feedback-based OPF algorithms in distribution networks, and also to improve performance of algorithms that make use of "pseudo-measurements", we integrate a state estimation algorithm based on a sparse set of available measurements, before performing the dual variable update (6d). This allows us to utilize improved information on the network state to make decisions, specifically improving information at "blind spots" of the grid where there are no direct measurements. Fig. 2 illustrates the proposed OPF framework with state estimation in-the-loop.

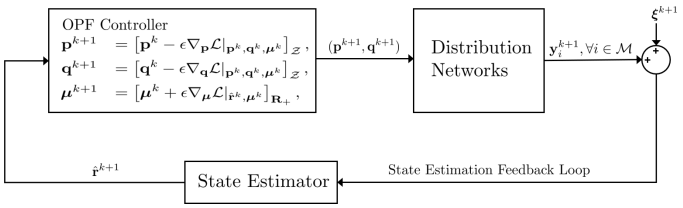

Fig. 2. The diagram of the proposed optimal power flow problem with SE in-the-loop.

C. State Estimation In-the-Loop

We consider the grid measurement model

$$\mathbf{y}^k = h(\mathbf{r}^k) + \boldsymbol{\xi}^k, \tag{12}$$

where $\mathbf{r}^k \in \mathbf{R}^M$ is the system state at time k, $\mathbf{y}^k \in \mathbf{R}^L$ is a measurement vector received at time k comprising raw noisy measurements from sensors and pseudo-measurements (which include real and reactive power injections, real and reactive power flow, and voltage magnitude and angles), and $h : \mathbf{R}^M \to \mathbf{R}^L$ is a measurement function. The vector $\boldsymbol{\xi}^k \in \mathbf{R}^L$ models measurement error, assumed iid according to a Gaussian distribution $N(0, \Sigma), \Sigma \in \mathbf{R}^{L\times L}$. The pseudo-measurements are modeled as sensor measurements corrupted by high-variance Gaussian noise based on historical data (e.g., customer billing data and typical load profile) that provide rough information about variations in the state of the grid [31].

To estimate grid states from the available measurements, we consider the WLS estimator [16], [31], [39]:

$$\hat{\mathbf{r}}^k = \underset{\mathbf{r}^k}{\operatorname{argmin}} \frac{1}{2}\left(\mathbf{y}^k - h(\mathbf{r}^k)\right)^\intercal W \left(\mathbf{y}^k - h(\mathbf{r}^k)\right), \tag{13}$$

where the weight matrix is defined as $W = \Sigma^{-1}$. The actual state $\mathbf{r}^k = f(\mathbf{p}^k, \mathbf{q}^k)$ is uniquely determined by the network power flow. Existence and uniqueness of a solution to (13) require certain properties of the measurement function.

Definition 1 (Full Observability[4] [24], [40])**.** *The system state is called fully observable if* $\mathbf{r}^k = 0$ *is the only solution for* $h(\mathbf{r}^k) = 0$*, which allows a unique solution to* (13)*.*

Assumption 4. *We assume that the distribution system state with measurements* (12) *is fully observable.*

Since distribution networks typically have only a sparse set of real-time measurements from deployed sensors, we require enough pseudo-measurements to ensure full observability. It is always possible to include enough pseudo-measurements to ensure full observability and satisfy Assumption 4. The effectiveness combining real measurements and pseudo-measurements has been observed in [39], [41].

Fig. 2 and Algorithm 1 illustrate and describe the proposed OPF controller with the state-estimation feedback loop. Note that the step 2 in Algorithm 1 is not implemented in the proposed OPF controller, but instead is a realization of the power

[4]This definition should be distinguished from observability of linear dynamical systems. Here, we limit the definition of observability to power system static state estimation problems [26] throughout this manuscript.

Algorithm 1 (OPF with SE In-the-Loop)

Require: netload initialization $(\mathbf{p}^0, \mathbf{q}^0)$ and $\boldsymbol{\mu}^k$

1: **for** $k = 0 : K$ **do**
2: $\quad \mathbf{r}^k \leftarrow$ nonlinear power flow $(\mathbf{p}^k, \mathbf{q}^k)$
3: $\quad$ receive system measurement $\mathbf{y}^k$
4: $\quad$ SE of all electrical quantities of interest $\hat{\mathbf{r}}^k$
5: $\quad \mathbf{p}^{k+1} = \left[\mathbf{p}^k - \epsilon \nabla_{\mathbf{p}} \mathcal{L}(\mathbf{p}^k, \mathbf{q}^k, \boldsymbol{\mu}^k)\right]_{\mathcal{Z}}$
6: $\quad \mathbf{q}^{k+1} = \left[\mathbf{q}^k - \epsilon \nabla_{\mathbf{q}} \mathcal{L}(\mathbf{p}^k, \mathbf{q}^k, \boldsymbol{\mu}^k)\right]_{\mathcal{Z}}$
7: $\quad \boldsymbol{\mu}^{k+1} = \left[\boldsymbol{\mu}^k + \epsilon \nabla_{\boldsymbol{\mu}} \mathcal{L}(\hat{\mathbf{r}}^k, \boldsymbol{\mu}^k)\right]_{\mathbf{R}_+}$
8: **end for**

system state's physical response $\mathbf{r}^k$ resulting from gradient updates on nodal power injections $(\mathbf{p}^k, \mathbf{q}^k)$. We utilize SE in-the-loop to compute a state estimate $\hat{\mathbf{r}}^k$, which then contributes to the update of dual variables μ^{k+1} in step 7. Our numerical experiments in Section IV compare this approach with the direct use of noisy measurements and pseudo-measurements without an estimation scheme.

D. Convergence Analysis

The computations and updates in steps 5-7 of Algorithm 1 are written more explicitly as

$$\hat{\mathbf{r}}^k = \underset{\mathbf{r}^k}{\operatorname{argmin}} \frac{1}{2} \left(\mathbf{y}^k - h(\mathbf{r}^k)\right)^{\intercal} W \left(\mathbf{y}^k - h(\mathbf{r}^k)\right), \tag{14a}$$

$$\mathbf{p}^{k+1} = \left[\mathbf{p}^k - \epsilon \left(\nabla_{\mathbf{p}} C(\mathbf{p}^k, \mathbf{q}^k) + \nabla_{\mathbf{p}} C_0(\mathbf{p}^k, \mathbf{q}^k) + \mathbf{A}^{\intercal} \boldsymbol{\mu}^k\right)\right]_{\mathcal{Z}}, \tag{14b}$$

$$\mathbf{q}^{k+1} = \left[\mathbf{q}^k - \epsilon \left(\nabla_{\mathbf{q}} C(\mathbf{p}^k, \mathbf{q}^k) + \nabla_{\mathbf{q}} C_0(\mathbf{p}^k, \mathbf{q}^k) + \mathbf{B}^{\intercal} \boldsymbol{\mu}^k\right)\right]_{\mathcal{Z}}, \tag{14c}$$

$$\boldsymbol{\mu}^{k+1} = \left[\boldsymbol{\mu}^k + \epsilon \left(\mathbf{g}(\hat{\mathbf{r}}^k) - \eta \boldsymbol{\mu}^k\right)\right]_{\mathbf{R}_+}, \tag{14d}$$

This iteration (14) is performed until convergence.

As the state estimation in distribution networks has been widely discussed for different applications [27], the existing literature shows that these type of methods lead to an accurate and computationally efficient approximation under nominal operating condition. We also define other two mappings: the SE in-the-loop operator $\overline{\Phi}(\mathbf{x}^k)$, where the gradient updates based on SE results $\hat{\mathbf{r}}^k$ from (13) to update the dual variables

$$\overline{\Phi} : \{\mathbf{p}^k, \mathbf{q}^k, \boldsymbol{\mu}^k\} \mapsto \begin{bmatrix} \epsilon \nabla_{\mathbf{p}} \mathcal{L}|_{\mathbf{p}^k, \mathbf{q}^k, \boldsymbol{\mu}^k} \\ \epsilon \nabla_{\mathbf{q}} \mathcal{L}|_{\mathbf{p}^k, \mathbf{q}^k, \boldsymbol{\mu}^k} \\ -\epsilon \nabla_{\boldsymbol{\mu}} \mathcal{L}|_{\hat{\mathbf{r}}^k, \boldsymbol{\mu}^k} \end{bmatrix}.$$

Since the sensor measurement $\mathbf{y^k}$ inherit from the nonlinear physical system response (11), we use the nonlinear power flow mapping $\tilde{\Phi}(\mathbf{x}^k)$ to capture these difference,

$$\tilde{\Phi} : \{\mathbf{p}^k, \mathbf{q}^k, \boldsymbol{\mu}^k\} \mapsto \begin{bmatrix} \epsilon \nabla_{\mathbf{p}} \mathcal{L}|_{\mathbf{p}^k, \mathbf{q}^k, \boldsymbol{\mu}^k} \\ \epsilon \nabla_{\mathbf{q}} \mathcal{L}|_{\mathbf{p}^k, \mathbf{q}^k, \boldsymbol{\mu}^k} \\ -\epsilon \nabla_{\boldsymbol{\mu}} \mathcal{L}|_{\mathbf{r}^k = f(\mathbf{p}^k, \mathbf{q}^k), \boldsymbol{\mu}^k} \end{bmatrix}.$$

Assumption 5. *There is a uniform bound on the squared error of the gradient update due to state estimation, i.e., there exists $\alpha > 0$ such that*

$$\mathbf{E}\left[\|\Phi(\mathbf{x}^k) - \overline{\Phi}(\mathbf{x}^k)\|_2^2\right] = \sigma_k^2 \leq \alpha, \quad \forall \mathbf{x}^k. \tag{15}$$

Assumption 6. *There is a uniform bound on the norm of the squared distance between update with SE in-the-loop and the update that uses the actual nonlinear power flow in (11), i.e., there exists $\rho > 0$ such that*

$$\|\overline{\Phi}(\mathbf{x}^k) - \tilde{\Phi}(\mathbf{x}^k)\|_2^2 \leq \rho, \quad \forall \mathbf{x}^k. \tag{16}$$

Definition 2. *The estimation error variance from SE in-the-loop of the saddle point of (5) is defined as*

$$\sigma_*^2 := \mathbf{E}\left[\|\Phi(\mathbf{x}^*) - \overline{\Phi}(\mathbf{x}^*)\|_2^2\right].$$

Theorem 2. *Suppose the step size ϵ satisfies the condition (10) from Theorem 1. Under Assumptions 5-6, the sequence $\{\mathbf{x}^k\}$ generated by Algorithm 1 satisfies*

$$\lim_{k \to \infty} \sup \mathbf{E}\left[\|\mathbf{x}^k - \mathbf{x}^*\|_2^2\right] = \frac{\epsilon^2 \left(\rho + 2\sigma_*^2 + \alpha\right)}{2\epsilon M - \epsilon^2 L^2}, \tag{17}$$

where $\mathbf{x}^* = [(\mathbf{p}^*)^{\intercal}, (\mathbf{q}^*)^{\intercal}, (\boldsymbol{\mu}^*)^{\intercal}]^{\intercal}$ is saddle point of $\mathcal{L}$ in (5).

Proof. See proof in the Appendix. □

The condition (17) from Theorem 2 provides an upper bound on the expected squared distance between the sequence $\{\mathbf{x}^k | \ \mathbf{x}^k := [(\mathbf{p}^k)^{\intercal}, (\mathbf{q}^k)^{\intercal}, (\boldsymbol{\mu}^k)^{\intercal}]^{\intercal}, k \leq K, K \to \infty\}$ generated by our proposed OPF with SE feedback algorithm (14) and the saddle point $\mathbf{x}^*$ of (5). This analytical bound indicates that our proposed approach has robust performance to estimation errors and measurement noise.

1) *Inherent measurement noise:* The online measurements by PMUs are typically within $1\% \sim 2\%$ of actual values. The pseudo measurements of active and reactive power can be regarded as a rough initialization (with up to 50% variations in comparison to actual values). These errors can be reduced through the estimation phase in (13), which improves decisions from the OPF controller with SE feedback (14a), improving robustness to measurement noise and power variability;

2) *Linearization approximation errors:* The OPF-phase (and some of state estimators) in the proposed algorithm utilize the linearized power flow to promote computational efficiency in gradient calculation. The discrepancy between linearized and nonlinear power flow is quantified in (16) by ρ, when set-points $(\mathbf{p}^k, \mathbf{q}^k)$ are realized by the nonlinear network power flow.

E. Estimation Error Analysis

In this subsection, we analytically quantify the errors of the SE algorithm under a linearized measurement model. A linear measurement model is given by

$$\mathbf{y}^k = H\mathbf{r}^k + \boldsymbol{\xi}^k,$$

where $H \in \mathbf{R}^{L \times M}$ is a measurement matrix that could be obtained by linearizing the nonlinear measurement function around a particular nominal operating condition.

For the linear WLS problem

$$\min_{\mathbf{r}^k} \frac{1}{2} \left(\mathbf{y}^k - H\mathbf{r}^k\right)^{\intercal} W \left(\mathbf{y}^k - H\mathbf{r}^k\right),$$

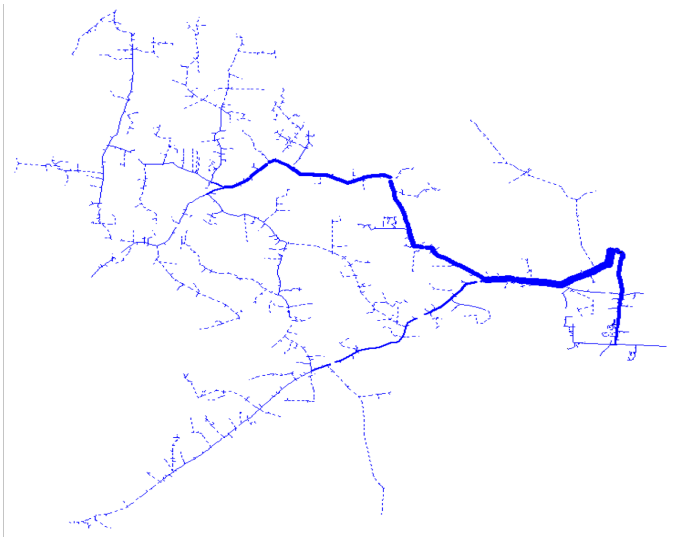

Fig. 3. A 11,000-node distribution network. This testbed is constructed by connecting an IEEE 8,500-node distribution network and an EPRI Ckt7 test feeder at PCC. The primary side of this modified feeder is modelled in detail, while the loads on secondary side are merged into distribution transformers. This lumps the 11,000-node testbed into a 4521-node distribution network.

the closed-form analytical solution is given by $\hat{\mathbf{r}}^k = (H^\intercal W H)^{-1} H^\intercal W \mathbf{y}^k$. When the matrix $H^\intercal W H$ is non-singular (which occurs when W is positive definite and H is full column rank), then the estimate can be expressed as

$$\begin{aligned}\hat{\mathbf{r}}^k &= (H^\intercal W H)^{-1} H^\intercal W H \mathbf{r}^k + (H^\intercal W H)^{-1} H^\intercal W \boldsymbol{\xi}^k \\ &= \mathbf{r}^k + (H^\intercal W H)^{-1} H^\intercal W \boldsymbol{\xi}^k.\end{aligned}$$

The WLS estimator is unbiased (since $\mathbf{E}\left[\hat{\mathbf{r}}^k\right] = \mathbf{r}^k$ due to the noise being zero mean), and the variance is given by $\text{Var}\left[\hat{\mathbf{r}}_j^k\right] = \sum_{i=1}^n \Gamma_{ji}\sigma_i^2$, where Γ_{ji} denotes the ji-th element of the $\Gamma = (H^\intercal W H)^{-1} H^\intercal W$, and σ_i^2 is the ith diagonal of the measurement covariance matrix Σ. Confidence intervals for components of the state estimate $\hat{\mathbf{r}}^k$ can be constructed as

$$\hat{\mathbf{r}}_j^k \pm c\sqrt{\text{Var}\left(\hat{\mathbf{r}}_j^k\right)} = \hat{\mathbf{r}}_j^k \pm c\sqrt{\sum_{i=1}^n \Gamma_{ji}\sigma_i^2},$$

where c can be chosen based on the prescribed confidence level. In addition to the bound in Theorem 2, the confidence intervals provide a numerical performance metric on the severity of estimation errors within the OPF control loop. In the next section, we will use this analysis to quantify estimation errors from voltage measurements and netoad pseudo-measurements.

IV. Numerical Results

In this section, we use a modified three-phase unbalanced 11,000-node distribution network shown in Fig. 3 to demonstrate the effectiveness and scalability of the proposed OPF solver with SE in-the-loop. We model the primary loads of this system in detail and merge the secondary loads into distribution transformers, which lumps the system into a 4521-node distribution network. This extremely large system is divided into 5 clusters and then we utilized a spatially distributed

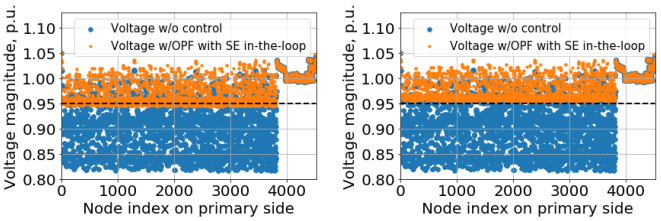

(a) normal bound (b) tighter bound

Fig. 4. Voltage profile of OPF controller with SE in-the-loop. The black dash line indicates the lower voltage bound, i.e., 0.95 p.u.. After we utilize a tighter bound $[0.96, 1.05]$ to compensates the inherent errors of SE in-the-loop, the voltage profile on the right then meets the constraint.

optimization algorithm for computational affordability. The details of multi-phase power flow modelling and the feasibility of distributed algorithm were discussed in our companion paper [32]. Here, we focus on closing a loop between OPF and SE to solve a general OPF problem. We explore a tradeoff between sensing and communication effectiveness and performance of OPF controllers in an extremely large network.

We consider a voltage regulation problem where the state is voltage magnitude. In particular, we define the state as the voltage magnitude vector $\mathbf{r} := |\mathbf{v}| := [|v_1|, \ldots, |v_N|]^\intercal \in \mathbf{R}_{++}^N$ and consider

$$\begin{aligned}\textbf{OPF-V:} \quad \min_{\mathbf{p},\mathbf{q},|\mathbf{v}|} \quad & \sum_{i\in\mathcal{N}} C_i(p_i, q_i) + C_0(\mathbf{p}, \mathbf{q}), \\ \text{s.t.} \quad & |\mathbf{v}| = \mathbf{A}\mathbf{p} + \mathbf{B}\mathbf{q} + |\mathbf{v}_0|, \\ & \underline{\mathbf{v}} \le |\mathbf{v}| \le \bar{\mathbf{v}}, \\ & (p_i, q_i) \in \mathcal{Z}_i, \forall i \in \mathcal{N}.\end{aligned}$$

The inequality constraints capture the lower and upper bounds $(\underline{\mathbf{v}}, \bar{\mathbf{v}})$ of voltage magnitudes. In particular, we take linear approximation for AC power flow to express $|\mathbf{v}|$ as a linear function of power injection $(\mathbf{p}, \mathbf{q})$. The coefficient matrics $(\mathbf{A}, \mathbf{B})$ of the linearized voltages and normalized vector $|\mathbf{v}_0|$ can be attained from numerous linearization methods, e.g., [33], [35], [42]. The gradient-based OPF controller (14) utilizes the online voltage magnitude measurement and voltage estimation to make the system converge.

The default voltage profile of system in Fig. 3 without any control[5] is given by OpenDSS [43] shown in blue dots in Fig. 4. The voltage limits $\bar{\mathbf{v}}$ and $\underline{\mathbf{v}}$ are set to 1.05 and 0.95 p.u. This particular network has a significant under-voltage situation. To have a clear picture of voltage level for OPF controller, most of the literature assumes that we have full knowledge of the real-time voltage information, which requires an unrealistic sensor deployment, extreme communication, and huge investment. To tradeoff these two issues and facilitate a practical OPF controller for acceptable performance, we randomly deploy voltage magnitude measurements at 3.6% of the nodes with measurement noise subject to Gaussian distribution with zero mean and 1% standard deviation. We also

[5]We disable all rule-based control of voltage regulators, local capacitors and low-voltage transformers, etc., and then only solve the nonlinear power flow.

have the load pseudo-measurements for all nodal injections (i.e., active and reactive power) with significant noise (e.g., zero mean and 50% standard deviation of real values), which will guarantee the full observability of SE in-the-loop. The voltage information of the whole network will be fed back to OPF controller based on the voltage estimation results. The simulation is conducted on a desktop with AMD Ryzen 7 2700X Eight-Core Processor CPU@3.7GHz, 64GM RAM, Python 3.7 and Windows 10.

Fig. 4 visualizes the voltage profile regulated by the OPF controller with SE in-the-loop. In order to prevent voltage from failing below 0.95 p.u., the netloads must be curtailed based on the SE feedback information. The voltage of most nodes (i.e., orange dots) have been bounded within $[0.95, 1.05]$. There are few voltages just located across the lower bound with slight variations. This is due to the feedback signal containing the voltage estimation errors. To understand the severity of these estimation errors due to sensor noise and large variation of pseudo measurement, we use the analysis in Section III-E to quantify the statistical estimation error numerically. Fig. 5 and Fig. 6 visualize the average and maximum errors of voltage estimation, and the comparison with analytically calculated confidence intervals over each OPF gradient step. Most of average errors over 1000 OPF iterations are bounded by the 99% confidence interval. Based on the numerical analysis in Fig. 5, we conclude that having SE in-the-loop will significantly reduce errors due to inherent measurement noise compared to direct use of raw measurements. Also, the proposed SE in-the-loop can mitigates the effects of measurement errors on OPF controller performance.

To resolve the feedback estimation errors and further improve the performance of OPF controllers, we give a tighter lower bound (i.e., $[0.96, 1.05]$) based on the statistical analysis of SE errors. As a result shown in Fig. 7, the network curtails more netloads to achieve a more conservative voltage profile, which leads to a higher operational cost. We emphasize that there is always a tradeoff between: 1) cost of the measurement system (e.g., number of deployed sensors, communication infrastructure) and 2) OPF controller performance (e.g., robustness, feasibility and optimality). In general, our proposed approach provides utilities and system operators a framework to systematically design OPF controllers under a limited set of sensor measurements.

Overall, we conclude that the proposed OPF controller with SE feedback is able to systemically reduce estimation error of voltages at unmeasured nodes, successfully achieve voltage regulation, and improve robustness to measurement and estimation errors. The benefits of closing the loop between OPF controllers and state estimators can be clearly observed from the perspectives of effectiveness, robustness and efficiency.

V. Conclusions and Outlooks

In this paper, we proposed a general optimal power flow controller with state estimation feedback to facilitate the operation of modern distribution networks. The controller depends explicitly on the state estimation results derived from system measurements. In contrast to existing works, our method

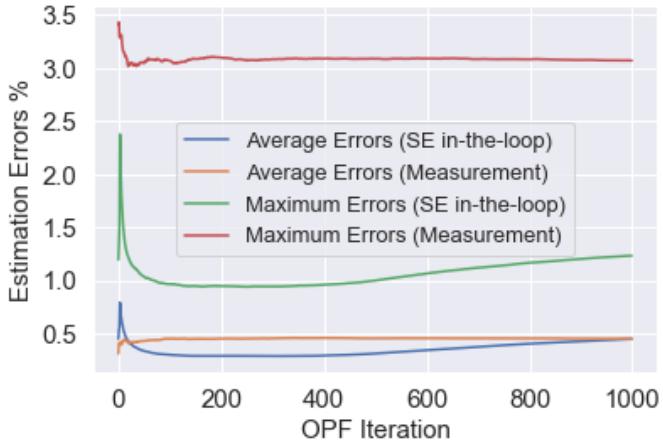

Fig. 5. Comparison of estimation errors between SE in-the-loop and the use of raw voltage measurements. The running average of average/maximum errors show that the SE in-the-loop yields less error than using raw measurements.

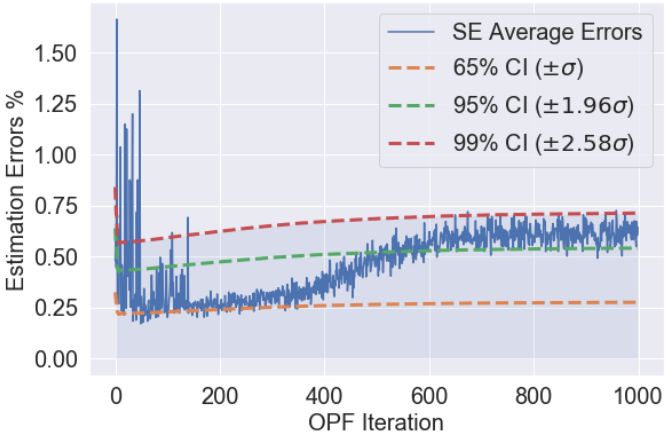

Fig. 6. Comparison of the average estimation errors with different confidence intervals over 1000 OPF iterations.

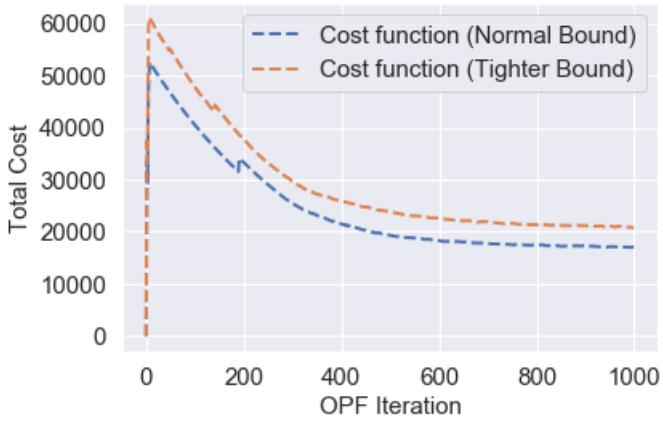

Fig. 7. Total cost with SE in-the-loop over 1000 OPF iterations.

utilizes a feedback loop to the OPF controller to estimate the system voltages from a limited number of sensors rather than making strong assumptions on full observability or requiring full state measurements. The performance of our design is analyzed and numerically demonstrated. The numerical results demonstrate the effectiveness, scalability, and robustness of the proposed OPF controller with SE in-the-loop.

Our results on OPF problem launched an initial step towards closing a loop between control and state estimation in power systems. There are several lines of future works that can extend the present results in various ways to more fully explore the benefits, and discover the limitations of having SE in-the-loop for OPF controllers. Future work includes

- performance evaluation of various OPF formulations with different SE techniques in-the-loop;
- optimal sensor placement with SE in-the-loop for better OPF performance;
- OPF & SE in-the-loop co-design considering the estimation errors for a more efficient communication structure in a real network.

ACKNOWLEDGEMENT

We would like to thank Mr. Zhiyuan Liu from Department of Computer Science, The University of Colorado at Boulder, for his support on the simulation testbed construction.

This work was authored in part by the National Renewable Energy Laboratory, operated by Alliance for Sustainable Energy, LLC, for the U.S. Department of Energy (DOE) under Contract No. DE-EE-0007998. Funding provided by U.S. Department of Energy Office of Energy Efficiency and Renewable Energy Solar Energy Technologies Office. The views expressed in the article do not necessarily represent the views of the DOE or the U.S. Government. The U.S. Government retains and the publisher, by accepting the article for publication, acknowledges that the U.S. Government retains a nonexclusive, paid-up, irrevocable, worldwide license to publish or reproduce the published form of this work, or allow others to do so, for U.S. Government purposes.

REFERENCES

[1] J. Carpentier, "Contribution to the economic dispatch problem," *Bulletin de la Societe Francaise des Electriciens*, vol. 3, no. 8, pp. 431–447, 1962.

[2] H. W. Dommel and W. F. Tinney, "Optimal power flow solutions," *IEEE Transactions on Power Apparatus and Systems*, pp. 1866–1876, Oct. 1968.

[3] O. Alsac and B. Stott, "Optimal load flow with steady-state security," *IEEE Transactions on Power Apparatus and Systems*, pp. 745–751, May 1974.

[4] R. Baldick, B. H. Kim, C. Chase, and Y. Luo, "A fast distributed implementation of optimal power flow," *IEEE Transactions on Power Systems*, vol. 14, pp. 858–864, Aug. 1999.

[5] S. H. Low, "Convex relaxation of optimal power flow, Part I: Formulations and equivalence," *IEEE Transactions on Control of Network Systems*, vol. 1, pp. 15–27, March 2014.

[6] A.-H. Mohsenian-Rad, V. W. Wong, J. Jatskevich, R. Schober, and A. Leon-Garcia, "Autonomous demand-side management based on game-theoretic energy consumption scheduling for the future smart grid," *IEEE Transactions on Smart Grid*, vol. 1, no. 3, pp. 320–331, 2010.

[7] D. S. Callaway and I. A. Hiskens, "Achieving controllability of electric loads," *Proceedings of the IEEE*, vol. 99, no. 1, pp. 184–199, 2010.

[8] E. F. Camacho, T. Samad, M. Garcia-Sanz, and I. Hiskens, "Control for renewable energy and smart grids," *The Impact of Control Technology, Control Systems Society*, pp. 69–88, 2011.

[9] S. Maharjan, Q. Zhu, Y. Zhang, S. Gjessing, and T. Basar, "Dependable demand response management in the smart grid: A stackelberg game approach," *IEEE Transactions on Smart Grid*, vol. 4, no. 1, pp. 120–132, 2013.

[10] A. Bernstein, C. Wang, E. DallAnese, J.-Y. Le Boudec, and C. Zhao, "Load flow in multiphase distribution networks: Existence, uniqueness, non-singularity and linear models," *IEEE Transactions on Power Systems*, vol. 33, no. 6, pp. 5832–5843, 2018.

[11] T. Summers, J. Warrington, M. Morari, and J. Lygeros, "Stochastic optimal power flow based on conditional value at risk and distributional robustness," *International Journal of Electrical Power & Energy Systems*, vol. 72, pp. 116–125, 2015.

[12] H.-D. Chiang and M. E. Baran, "On the existence and uniqueness of load flow solution for radial distribution power networks," *IEEE Transactions on Circuits and Systems*, vol. 37, no. 3, pp. 410–416, 1990.

[13] P. Piagi and R. H. Lasseter, "Autonomous control of microgrids," in *IEEE Power Engineering Society General Meeting*, 2006.

[14] P. Palensky and D. Dietrich, "Demand side management: Demand response, intelligent energy systems, and smart loads," *IEEE Transactions on Industrial Informatics*, vol. 7, no. 3, pp. 381–388, 2011.

[15] D. K. Molzahn, I. A. Hiskens, *et al.*, "A survey of relaxations and approximations of the power flow equations," *Foundations and Trends® in Electric Energy Systems*, vol. 4, no. 1-2, pp. 1–221, 2019.

[16] F. F. Wu, "Power system state estimation: A survey," *International Journal of Electrical Power & Energy Systems*, vol. 12, no. 2, pp. 80–87, 1990.

[17] M. Abido, "Optimal power flow using particle swarm optimization," *International Journal of Electrical Power & Energy Systems*, vol. 24, no. 7, pp. 563–571, 2002.

[18] M. Colombino, E. Dall'Anese, and A. Bernstein, "Online optimization as a feedback controller: Stability and tracking," *IEEE Transactions on Control of Network Systems*, 2019.

[19] X. Zhou, E. DallAnese, L. Chen, and A. Simonetto, "An incentive-based online optimization framework for distribution grids," *IEEE Transactions on Automatic Control*, vol. 63, no. 7, pp. 2019–2031, 2017.

[20] E. DallAnese and A. Simonetto, "Optimal power flow pursuit," *IEEE Transactions on Smart Grid*, vol. 9, no. 2, pp. 942–952, 2016.

[21] P. Li, H. Wang, and B. Zhang, "A distributed online pricing strategy for demand response programs," *IEEE Transactions on Smart Grid*, Aug. 2017.

[22] J. Liu, J. Tang, F. Ponci, A. Monti, C. Muscas, and P. A. Pegoraro, "Trade-offs in PMU deployment for state estimation in active distribution grids," *IEEE Transactions on Smart Grid*, vol. 3, no. 2, pp. 915–924, 2012.

[23] K. Dehghanpour, Y. Yuan, Z. Wang, and F. Bu, "A game-theoretic data-driven approach for pseudo-measurement generation in distribution system state estimation," *IEEE Transactions on Smart Grid*, 2019.

[24] A. Abur and A. G. Exposito, *Power system state estimation: theory and implementation*. CRC press, 2004.

[25] K. Dehghanpour, Z. Wang, J. Wang, Y. Yuan, and F. Bu, "A survey on state estimation techniques and challenges in smart distribution systems," *IEEE Transactions on Smart Grid*, vol. 10, no. 2, pp. 2312–2322, 2018.

[26] F. C. Schweppe and J. Wildes, "Power system static-state estimation, Part I-III," *IEEE Transactions on Power Apparatus and Systems*, no. 1, pp. 120–135, 1970.

[27] A. Primadianto and C.-N. Lu, "A review on distribution system state estimation," *IEEE Transactions on Power Systems*, vol. 32, no. 5, pp. 3875–3883, 2016.

[28] F. Ahmad, A. Rasool, E. Ozsoy, R. Sekar, A. Sabanovic, and M. Elitaş, "Distribution system state estimation-a step towards smart grid," *Renewable and Sustainable Energy Reviews*, vol. 81, pp. 2659–2671, 2018.

[29] A. S. Zamzam, X. Fu, and N. D. Sidiropoulos, "Data-driven learning-based optimization for distribution system state estimation," *IEEE Transactions on Power Systems*, 2019.

[30] Y. Guo, X. Zhou, C. Zhao, Y. Chen, T. Summers, and L. Chen, "Solving optimal power flow for distribution networks with state estimation feedback," in *Annual American Control Conference*, pp. 1–8, July 2020.

[31] A. Gomez-Exposito and A. Abur, *Power System State Estimation: Theory and Implementation*. CRC press, 2004.

[32] X. Zhou, Z. Liu, C. Zhao, and L. Chen, "Accelerated voltage regulation in multi-phase distribution networks based on hierarchical distributed algorithm," *IEEE Transactions on Power Systems*, 2020.

[33] A. Bernstein and E. Dall'Anese, "Linear power-flow models in multiphase distribution networks," in *IEEE PES Innovative Smart Grid Technologies Conference Europe*, 2017.

[34] S. Bolognani and F. Dörfler, "Fast power system analysis via implicit linearization of the power flow manifold," in *IEEE Annual Allerton Conference on Communication, Control, and Computing*, pp. 402–409, 2015.

[35] L. Gan and S. H. Low, "An online gradient algorithm for optimal power flow on radial networks," *IEEE Journal on Selected Areas in Communications*, vol. 34, no. 3, pp. 625–638, 2016.

[36] M. E. Baran and F. F. Wu, "Network reconfiguration in distribution systems for loss reduction and load balancing," *IEEE Transactions on Power Delivery*, vol. 4, no. 2, pp. 1401–1407, 1989.

[37] J. Koshal, A. Nedić, and U. V. Shanbhag, "Multiuser optimization: Distributed algorithms and error analysis," *SIAM Journal on Optimization*, vol. 21, no. 3, pp. 1046–1081, 2011.

[38] A. Bernstein, L. Reyes-Chamorro, J.-Y. Le Boudec, and M. Paolone, "A composable method for real-time control of active distribution networks with explicit power setpoints. Part I: Framework," *Electric Power Systems Research*, vol. 125, pp. 254–264, 2015.

[39] X. Zhou, Z. Liu, Y. Guo, C. Zhao, and L. Chen, "Gradient-based multi-area distribution system state estimation," *arXiv preprint, arXiv:1909.11266*, 2019.

[40] F. F. Wu and A. Monticelli, "Network observability: theory," *IEEE Transactions on Power Apparatus and Systems*, no. 5, pp. 1042–1048, 1985.

[41] I. Džafić, M. Gilles, R. A. Jabr, B. C. Pal, and S. Henselmeyer, "Real time estimation of loads in radial and unsymmetrical three-phase distribution networks," *IEEE Transactions on Power Systems*, vol. 28, no. 4, pp. 4839–4848, 2013.

[42] M. E. Baran and F. F. Wu, "Optimal capacitor placement on radial distribution systems," *IEEE Transactions on Power Delivery*, vol. 4, no. 1, pp. 725–734, 1989.

[43] R. Dugan and R. Arritt, "The IEEE 8500-node test feeder," *Electric Power Research Institute, Palo Alto, CA, USA*, 2010.

APPENDIX

Recall $\mathbf{x}^k := [(\mathbf{p}^k)^\intercal, (\mathbf{q}^k)^\intercal, (\boldsymbol{\mu}^k)^\intercal]^\intercal$ and the primal-dual gradient mapping as

$$\Phi : \{\mathbf{p}^k, \mathbf{q}^k, \boldsymbol{\mu}^k\} \mapsto \begin{bmatrix} \epsilon \nabla_{\mathbf{p}} \mathcal{L}_\eta|_{\mathbf{p}^k,\mathbf{q}^k,\boldsymbol{\mu}^k} \\ \epsilon \nabla_{\mathbf{q}} \mathcal{L}_\eta|_{\mathbf{p}^k,\mathbf{q}^k,\boldsymbol{\mu}^k} \\ -\epsilon \nabla_{\boldsymbol{\mu}} \mathcal{L}|_{\mathbf{r}^k,\boldsymbol{\mu}^k} \end{bmatrix},$$

which is utilized to compute the gradient iterations of (6)

$$\mathbf{x}^{k+1} = \left[\mathbf{x}^k - \epsilon \Phi(\mathbf{x}^k)\right]_{\mathbf{R}_+ \times \mathcal{Z}},$$

where the dual variables are updated based on linearized power flow model (6a). We also define other two mappings: the SE in-the-loop operator $\overline{\Phi}(\mathbf{x}^k)$, where the gradient updates based on SE results $\hat{\mathbf{r}}^k$ from (13) to update the dual variables

$$\overline{\Phi} : \{\mathbf{p}^k, \mathbf{q}^k, \boldsymbol{\mu}^k\} \mapsto \begin{bmatrix} \epsilon \nabla_{\mathbf{p}} \mathcal{L}|_{\mathbf{p}^k,\mathbf{q}^k,\boldsymbol{\mu}^k} \\ \epsilon \nabla_{\mathbf{q}} \mathcal{L}|_{\mathbf{p}^k,\mathbf{q}^k,\boldsymbol{\mu}^k} \\ -\epsilon \nabla_{\boldsymbol{\mu}} \mathcal{L}|_{\hat{\mathbf{r}}^k,\boldsymbol{\mu}^k} \end{bmatrix}.$$

Since the sensor measurement $\mathbf{y}^\mathbf{k}$ inherit from the nonlinear physical system response (11), we use the nonlinear power flow mapping $\tilde{\Phi}(\mathbf{x}^k)$ to capture these difference,

$$\tilde{\Phi} : \{\mathbf{p}^k, \mathbf{q}^k, \boldsymbol{\mu}^k\} \mapsto \begin{bmatrix} \epsilon \nabla_{\mathbf{p}} \mathcal{L}|_{\mathbf{p}^k,\mathbf{q}^k,\boldsymbol{\mu}^k} \\ \epsilon \nabla_{\mathbf{q}} \mathcal{L}|_{\mathbf{p}^k,\mathbf{q}^k,\boldsymbol{\mu}^k} \\ -\epsilon \nabla_{\boldsymbol{\mu}} \mathcal{L}|_{\mathbf{r}^k = f(\mathbf{p}^k,\mathbf{q}^k),\boldsymbol{\mu}^k} \end{bmatrix},$$

then we have these assumptions, properties and definition

A1. There is a uniform bound on the squared error of the gradient update due to state estimation, i.e., there exists $\alpha > 0$ such that

$$\mathbf{E}\left[\|\Phi(\mathbf{x}^k) - \overline{\Phi}(\mathbf{x}^k)\|_2^2\right] = \sigma_k^2 \le \alpha, \quad \forall \mathbf{x}^k. \tag{19}$$

A2. There is a uniform bound on the norm of the squared distance between update with SE in-the-loop and the update that uses the actual nonlinear power flow in (11), i.e., there exists $\rho > 0$ such that

$$\|\overline{\Phi}(\mathbf{x}^k) - \tilde{\Phi}(\mathbf{x}^k)\|_2^2 \le \rho, \quad \forall \mathbf{x}^k. \tag{20}$$

In addition, the following properties can be observed based on our problem formulation,

B1. It can be shown [32] that Φ is strongly monotone and Lipschitz continuous, i.e., it satisfies for all feasible points $\mathbf{x}_1$ and $\mathbf{x}_2$ and for some constants $M > 0$ and $L > 0$

$$(\Phi(\mathbf{x}_1) - \Phi(\mathbf{x}_2))^\intercal (\mathbf{x}_1 - \mathbf{x}_2) \ge M \|\mathbf{x}_1 - \mathbf{x}_2\|_2^2, \tag{21}$$

$$\|\Phi(\mathbf{x}_1) - \Phi(\mathbf{x}_2)\|_2^2 \le L^2 \|\mathbf{x}_1 - \mathbf{x}_2\|_2^2. \tag{22}$$

D1. The estimation error variance from SE in-the-loop of the saddle point of (5) is defined as

$$\sigma_*^2 := \mathbf{E}\left[\|\Phi(\mathbf{x}^*) - \overline{\Phi}(\mathbf{x}^*)\|_2^2\right].$$

Proof of Theorem 2

Proof. Now we are ready to show convergence of OPF controller with SE in-the-loop. We have

$$\begin{aligned}
& \mathbf{E}\left[\|\mathbf{x}^{k+1} - \mathbf{x}^*\|_2^2\right] \\
\le\ & \mathbf{E}\left[\|\mathbf{x}^k - \epsilon\tilde{\Phi}(\mathbf{x}^k) - \mathbf{x}^* + \epsilon\Phi(\mathbf{x}^*)\|_2^2\right] \\
=\ & \mathbf{E}\Big[\|\mathbf{x}^k - \epsilon\tilde{\Phi}(\mathbf{x}^k) + \epsilon\overline{\Phi}(\mathbf{x}^k) - \epsilon\overline{\Phi}(\mathbf{x}^k) - \mathbf{x}^* + \epsilon\Phi(\mathbf{x}^*) \\
& + \epsilon\overline{\Phi}(\mathbf{x}^*) - \epsilon\overline{\Phi}(\mathbf{x}^*)\|_2^2\Big] \\
\le\ & \mathbf{E}\Big[\|\mathbf{x}^k - \epsilon\overline{\Phi}(\mathbf{x}^k) - \mathbf{x}^* + \epsilon\overline{\Phi}(\mathbf{x}^*)\|_2^2 + \epsilon^2\|\tilde{\Phi}(\mathbf{x}^k) - \overline{\Phi}(\mathbf{x}^k)\|_2^2 \\
& + \epsilon^2\|\Phi(\mathbf{x}^*) - \overline{\Phi}(\mathbf{x}^*)\|_2^2\Big] \\
=\ & \mathbf{E}\Big[\|\mathbf{x}^k - \epsilon\overline{\Phi}(\mathbf{x}^k) + \epsilon\Phi(\mathbf{x}^k) - \epsilon\Phi(\mathbf{x}^k) - \mathbf{x}^* + \epsilon\overline{\Phi}(\mathbf{x}^*) \\
& + \epsilon\Phi(\mathbf{x}^*) - \epsilon\Phi(\mathbf{x}^*)\|_2^2 + \epsilon^2\|\tilde{\Phi}(\mathbf{x}^k) - \overline{\Phi}(\mathbf{x}^k)\|_2^2 \\
& + \epsilon^2\|\Phi(\mathbf{x}^*) - \overline{\Phi}(\mathbf{x}^*)\|_2^2\Big] \\
\le\ & \mathbf{E}\left[\|\mathbf{x}^k - \epsilon\Phi(\mathbf{x}^k) - \mathbf{x}^* + \epsilon\Phi(\mathbf{x}^*)\|_2^2\right] \\
& + \mathbf{E}\left[\epsilon^2\|\overline{\Phi}(\mathbf{x}^k) - \Phi(\mathbf{x}^k)\|_2^2 + 2\epsilon^2\|\Phi(\mathbf{x}^*) - \overline{\Phi}(\mathbf{x}^*)\|_2^2\right] \\
& + \epsilon^2\|\tilde{\Phi}(\mathbf{x}^k) - \bar{\Phi}(\mathbf{x}^k)\|_2^2 \\
\le\ & \mathbf{E}\left[\|\mathbf{x}^k - \epsilon\Phi(\mathbf{x}^k) - \mathbf{x}^* + \epsilon\Phi(\mathbf{x}^*)\|_2^2\right] + \epsilon^2\left(\rho + \sigma_k^2 + 2\sigma_*^2\right) \\
\le\ & \mathbf{E}\left[\|\mathbf{x}^k - \mathbf{x}^*\|_2^2\right] + \mathbf{E}\left[\|\epsilon\Phi(\mathbf{x}^k) - \epsilon\Phi(\mathbf{x}^*)\|_2^2\right] \\
& - 2\epsilon\left(\Phi(\mathbf{x}^k) - \Phi(\mathbf{x}^*)\right)^\intercal\left(\mathbf{x}^k - \mathbf{x}^*\right) + \epsilon^2\left(\rho + \sigma_k^2 + 2\sigma_*^2\right) \\
\le\ & \left(\epsilon^2 L^2 - 2\epsilon M + 1\right)\mathbf{E}\left[\|\mathbf{x}^k - \mathbf{x}^*\|_2^2\right] + \epsilon^2\left(\rho + \sigma_k^2 + 2\sigma_*^2\right),
\end{aligned} \tag{23}$$

where the first inequality is due to non-expansiveness projection, the next two inequalities depend on the triangle inequality, the fourth inequality comes from (19),(20). The last two inequalities are due to the strong monotonicity (21) and Lipschitz continuity (22) of operator Φ. Now, we let $\Delta = \epsilon^2 L^2 - 2\epsilon M + 1$ and recursively implement the last inequality in (23) backwards to the initial step, then we have

$$\mathbf{E}\left[\|\mathbf{x}^K - \mathbf{x}^*\|_2^2\right]$$

$$\leq \Delta^K \|\mathbf{x}^0 - \mathbf{x}^*\|_2^2 + \epsilon^2 \left(\rho + 2\sigma_*^2\right) \left(\frac{1-\Delta^K}{1-\Delta}\right) + \epsilon^2 \sum_{k=0}^{K-1} \Delta^{K-1-k} \sigma_k^2 \tag{24a}$$

$$< \Delta^K \|\mathbf{x}^0 - \mathbf{x}^*\|_2^2 + \epsilon^2 \left(\rho + 2\sigma_*^2\right) \left(\frac{1-\Delta^K}{1-\Delta}\right) + \epsilon^2 \frac{1-\Delta^K}{1-\Delta} \alpha. \tag{24b}$$

By applying the SE estimation variance bound in Assumption 5, (24a) is relaxed to (24b). Then we have the step size chosen as $\epsilon < \frac{2M}{L}$ from Theorem 1, which leads to $0 < \Delta < 1$. As $K \to \infty$, Δ^K on the right-hand-side in (24b) will vanish. For such Δ and any initial condition $\mathbf{x}^0 \in \mathbf{R}$, when $K \to \infty$, the expectation of this discrepancy with be bounded by

$$\lim_{K \to \infty} \sup \mathbf{E}\left[\|\mathbf{x}^K - \mathbf{x}^*\|_2^2\right] = \frac{\epsilon^2 \left(\rho + 2\sigma_*^2 + \alpha\right)}{2\epsilon M - \epsilon^2 L^2},$$

which concludes the proof. □